International Journal of Environmental Research
https://doi.org/10.1007/s41742-018-0098-7

RESEARCH PAPER

Behavior of Natural Radionuclides, Radiological Hazard Parameters, and Magnetic Minerals in Rock Samples of Kolli Hills, Eastern Ghats, India

Nanjundan Krishnamoorthy[1] · Basavaraj Rachappa Kerur[2] · Sundaram Mullainathan[3] · Marcos Adrian Eduardo Chaparro[4] · Sugumaran Murugesan[5] · Mauro Alejandro Eduardo Chaparro[6]

Received: 4 November 2017 / Revised: 22 April 2018 / Accepted: 30 April 2018

Abstract

The natural radionuclide (^{238}U, ^{232}Th, and ^{40}K) content of the 15 rock samples collected from Kolli hills along the Eastern Ghats, India, has been analyzed using a $4'' \times 4''$ NaI (Tl) scintillation detector-based gamma-ray spectrometer. The activity concentrations of ^{238}U, ^{232}Th, and ^{40}K were between 12.97–49.89, 6.4–27.05, and 51.85–95.84 Bq kg^{-1}, respectively. To understand the entire radiological characteristics of the collected samples, the various radiological hazard parameters have been calculated and were compared with the global recommended mean values. From the magnetic studies, values of χ ranged from 33.1 to 510.7 $\times$ 10^{-8} m^3 kg^{-1}. Moreover, in rock samples of Kolli hills, ferrimagnetic minerals are found to be the main magnetic carrier. Statistical analyses were performed to study the relation between the natural radionuclides, radiological hazard parameters, and magnetic minerals. The results of Pearson's correlation analysis shows that ^{238}U and ^{232}Th strongly correlate with the radiological hazard parameters, and a poor correlation was noted between magnetic and radiological parameters. However, a positive and a near-positive correlation was also observed between SIRM/χ (0.501–0.578) and κ_{FD}% (0.471–0.481) with U and Th activity concentrations, respectively. This indicates that the carrier and grain size dependence parameters also play a significant role in increasing the activity concentrations of U and Th and its associated radiological parameters. From the cluster analysis, it is found that the content of ferrimagnetic minerals is higher in sample nos. 4, 5, 11, and 12, which greatly improves the properties of concrete when used for building construction purposes.

Keywords Natural radionuclides · Radiological hazard parameters · Magnetic minerals · Multivariate cluster analysis

✉ Nanjundan Krishnamoorthy
yenkrish.spectrum@gmail.com

[1] Department of Physics, CSI College of Engineering, Ketti 643 215, Tamilnadu, India

[2] Department of Physics, Gulbarga University, Gulbarga 585 106, Karnataka, India

[3] PG & Research Department of Physics, Thiru. Vi. Ka. Govt. Arts College, Thiruvarur 610 003, Tamilnadu, India

[4] Centro de Investigaciones en Física e Ingeniería del Centro de la Provincia de Buenos Aires (CIFICEN, CONICET-UNCPBA), Pinto 399, 7000 Tandil, Argentina

[5] Department of Physics, Sathyabama Institute of Science and Technology, Chennai 600 119, India

[6] Centro Marplatense de Investigaciones Matemáticas (CEMIM-UNMDP-CONICET), Diagonal J. B. Alberdi 2695, Mar del Plata, Argentina

Published online: 12 May 2018

Introduction

Humans living in the Earth's crust have always been exposed to natural ionizing radiations such as terrestrial and extra-terrestrial radiations. The origin of terrestrial radiation is due to the presence of naturally occurring radionuclides such as potassium and the decay chains of thorium and uranium, which is present in varying amounts in rock-forming minerals and soils; whereas extra-terrestrial radiation is due to high-energy cosmic-ray particles. It is well known that the Earth's surface is covered with rock and rock-forming minerals such as soil. Rocks and soils are the primary terrestrial sources of radiation in the environment that contribute to naturally occurring radionuclides (NOR). All rocks and soils are radioactive at different concentrations. They are composed of complex mixture that consists of various compounds such as minerals and organic matters. Since human beings are exposed to external gamma radiations in varying amounts depending upon their geology, it is of great interest to researchers to evaluate the concentration of natural radionuclides present in the environmental samples collected from that particular region (Gbadebo 2011; Olarinoye et al. 2010).

Environmental magnetism methods are rapid and non-destructive, and are commonly used to assess magnetic iron-mineral contents (Thompson and Oldfield 1986). In environmental magnetism, many techniques have been developed for determining the nature of the magnetic carriers in rocks, soils, and sediments. These techniques are used extensively to determine the magnetic properties of different materials. Since 1980, environmental magnetism has become a broad field that finds wide application in an ever increasing array of scientific disciplines (Verosub and Roberts 1995). These methods have been frequently used in diverse fields, including land-use studies, limnology, oceanography, sedimentology, and soil science, among many others.

Magnetic signals from rock, sediments, and soils are often dominated by ferromagnetic minerals sensu lato: ferrimagnetic (titano)-magnetite and/or antiferromagnetic hematite. These minerals are often not detected with standard analytical techniques due to their low concentrations ($< 1\%$ wt). However, magnetic measurements are sensitive enough to detect and identify such minerals, with concentrations that are several orders of magnitude smaller (Chaparro et al. 2014). The classification of magnetic components in natural samples in terms of mineralogy, domain state, and concentration is important for assessing the nature and origin of the components (Peters and Dekkers 2003).

It should be noted that the domination of ferromagnetic minerals in environmental samples such as rocks, soil, and sediments is due to the fact that they originate due to the disintegration of their parent rock during the process of pedogenesis, lithographic, and anthropogenic activities (Ramasamy et al. 2010). As a result, when rocks disintegrate naturally (for e.g., due to flow of the rain water), the natural radionuclides are carried over by the flow of water through the soil matter and finally they get deposited in stream, river, and other water bodies (Taskin et al. 2009). Therefore, it is clear that the concentration of natural radionuclides and magnetic minerals depends upon the parent rock. Multivariate statistics is adequate when attempting to determine the relationship between samples and/or between variables of the same or different nature. The determination of such relationships or groups (radionuclide and magnetic) is performed unbiased and with great statistical significance.

The aim of this study is to determine: (a) the relation between natural radionuclides, radiological hazard parameters and magnetic parameters; (b) relation among the various magnetic properties; and (c) groups of samples relative to magnetic parameters and the activity concentration of radionuclides.

Geology of the Study Area

Kolli hills are calm and pristine mountain range located about 55 km from Namakkal in the central part of Tamil Nadu on the Eastern Ghats of India (Fig. 1). On the north of Cauvery river, Kolli hills is the highest peak in Namakkal district with an elevation of about 1300 above mean sea level (Kumaresan et al. 2016). The altitude of the hill ranges from about 180 m (at the foot) to 1415 m (at the plateau) (Gurugnanam 2015). It is covered with evergreen forests that run almost parallel to the east coast of South India with a length of about 28 km along the north–south direction and 19 km wide along the east–west direction. The study area which covers a total area of 485 km^2 is geographically situated between the north latitudes 11°11′N–11°30′N and east longitudes 78°16′E–78°29′E, and is bounded by the Salem district on the northern side and Tiruchirappalli district in the eastern and the south eastern sides. The major portion of the hill area is occupied by structural hills (276.84 km^2); residual hills cover 0.48 km^2 in the northeastern region, whereas pediment covers an area of 23 km^2 in the northern, southern, and northeast regions. This report is based on satellite image mapping using remote sensing and geographic information system (GIS). The hill is also used for land use by humans where the hilltop geomorphology is noticed in western region covering an area of about 176.75 km^2 (Gurugnanam et al. 2014).

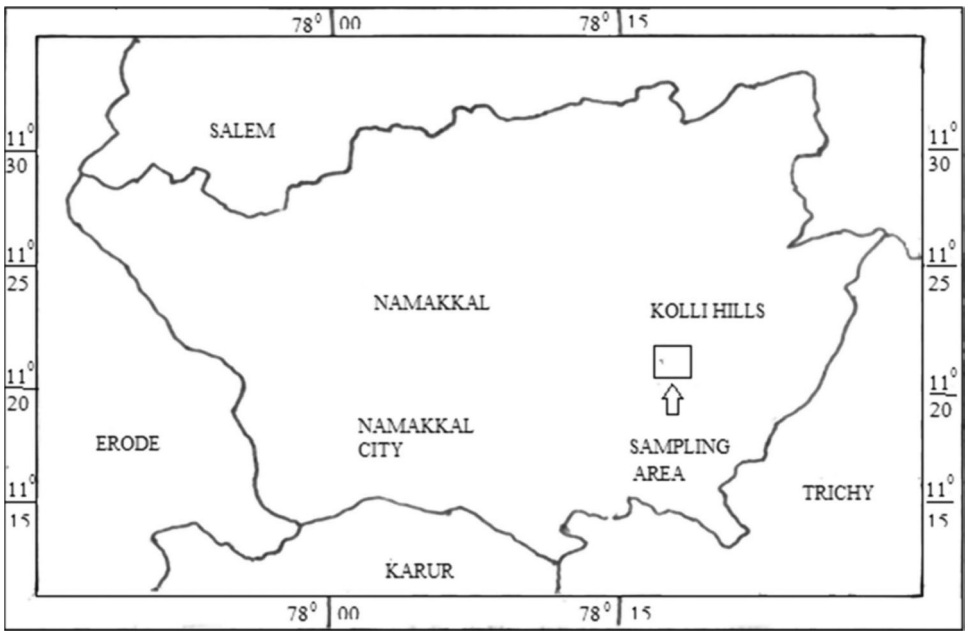

Fig. 1 Map of study area—Kolli hills, India

Materials and Methods

Sample Collection and Preparation

Rock samples were collected from 15 selected locations at various altitudes from the top of the Kolli hills toward its base. The collected rock samples were stored in thick polythene bags. Each sampling site was separated 100 m approximately. After collection, the samples were transported to the laboratory and kept at room temperature, crushed to powder, sieved using a 2 mm scientific mesh sieve, and dried in a hot air oven at 110 °C. The dried powdered rock samples were then packed and sealed in an airtight PVC container (250 ml), labeled and kept for a period of 4 weeks to allow radioactive equilibrium between radon (222Rn), thoron (220Rn), and their short-lived progenies to take place (Kurnaz et al. 2007).

Radioactivity Measurements

The activity concentrations of the primordial radionuclides ^{238}U, ^{232}Th, and ^{40}K in rock samples of Kolli hills were performed with a 4″ × 4″ NaI (Tl) scintillation detector-based gamma-ray spectrometer. To reduce the background level of the system that originates from the surrounding building materials and cosmic rays, the detector is shielded using 3″ thick lead bricks on all sides of the detector. To obtain gamma spectra of good statistics, the prepared rock samples were counted for a period of 60,000 s and the spectra are analyzed for the photo peak of uranium, thorium daughter products, and potassium. The gamma-ray spectrum was recorded using 1 K PC-based multichannel analyzer (winTMCA 32) with an inbuilt spectroscopic amplifier. Efficiency calibration of the system was carried out using the standards (uranium, thorium, and potassium) acquired from the International Atomic Energy Agency (IAEA). In the laboratory, gamma transitions of 1764, 2614, and 1460 keV gamma photo peaks emitted from ^{214}Bi, ^{208}Tl, and ^{40}K, respectively, were used for the measurement of activity concentrations. For each sample, the net count rate was calculated by subtracting the counts due to Compton scattering and also from other sources for the same counting time. The below detection limits (BDLs) for ^{238}U, ^{232}Th, and ^{40}K are 1.7, 3.1, and 7.9 Bq kg^{-1}, respectively.

Magnetic Measurements

Fifteen rock samples were subsampled for magnetic studies using plastic containers (2.3 cm^3). Dry samples were sieved (150 μm) to remove the fine fraction, and then they were packed, weighted, and labeled. Magnetic measurements were carried out in the Institute of Physics IFAS (Tandil, Argentina). Magnetic susceptibility measurements were performed using a magnetic susceptibility meter MS2, Bartington Instruments Ltd. (1994) linked to MS2B dual-frequency sensor (0.47 and 4.7 kHz). The magnetic susceptibility frequency dependence ($\kappa_{FD}\% = 100 \times [\kappa_{0.47kHz} - \kappa_{4.7kHz}]/\kappa_{0.47kHz}$) and mass-specific susceptibility (χ) were computed.

Remanent measurements such as anhysteretic remanent magnetization (ARM) and isothermal remanent magnetization (IRM) were done as well. The ARM was imparted using a partial ARM (pARM) device attached to a shielded

demagnetizer Molspin Ltd., superimposing a DC bias field of 90 μT to an AF of 100 mT and an AF decay rate of 17 μT per cycle. The remanent magnetization was measured by a spinner fluxgate magnetometer Minispin, Molspin Ltd. Anhysteretic susceptibility (volume κ_{ARM}, specific χ_{ARM}) was estimated using linear regression for ARM acquired at different DC bias fields (7.96 and 71.58 A/m). Related parameters, such as, King's plot (χ_{ARM} versus χ, King et al. 1982) and the ratio κ_{ARM}/κ (Dunlop and Özdemir 1997) were also calculated.

IRM studies were carried out using a pulse magnetizer model IM-10-30 ASC Scientific. Selected samples were magnetized by exposing it to DC fields, allowing it to increase up to 25 forward steps from 1.7 to 2470 mT. The remanent magnetization after each step was measured using the above-mentioned magnetometer Minispin. In these measurements, IRM acquisition curves and SIRM were found using forward DC fields. Remanent coercivity (H_{cr}, the backfield required to remove the SIRM, or IRM = 0) and S-ratio (= − IRM_{-300}/SIRM, where IRM_{-300} is the acquired IRM at a backfield of 300 mT) were also calculated from IRM measurement, using backfield once the SIRM was reached.

Statistical Analysis

Multivariate statistical analysis was performed using the R free software (R Core Team 2017) and was aimed to explore the relationship between the magnetic parameters (χ, ARM, SIRM, κ_{ARM}/κ ratio, ARM/SIRM, SIRM/χ, and H_{cr}) and activity concentration of the primordial radionuclides (^{238}U, ^{232}Th, and ^{40}K). Nonhierarchical k-means clustering (CA) was performed to build clusters of samples with similar magnetic and radionuclides features. Each of the clusters is characterized by both kinds of variables. The coordinates of the rows on the principal components (obtained from principal component analysis, PCA) were used to build the clusters. A very high percentage of the inertia (above 80%) should be retained by the components selected to obtain a stable and clear hierarchy.

For each cluster, a value of the reference is calculated to test the following null hypothesis (H0) "the average of x for category q is equal to the general average". This value is calculated as follows:

$$\text{v - test} = \frac{\bar{x}_q - \bar{x}}{\sqrt{\frac{s^2}{I_q}\frac{(I-I_q)}{(I-1)}}}, \quad (1)$$

where $\bar{x}_q$ is the average of variable x for the individuals of category q, $\bar{x}$ is the average of x for all of the individuals, and q is the number of individuals of the category.

Results and Discussion

Activity Concentration of Radionuclides

The activity concentrations of the sample were calculated from the peak intensity (cps) of each gamma line and the efficiency of the detector using the relation:

$$\text{Activity}\left(\text{Bq kg}^{-1}\right) = \frac{\text{Net area under the photopeak (cps)}}{\text{Efficiency}(\%)}. \quad (2)$$

The activity concentrations of the detected radionuclides ^{238}U, ^{232}Th, and ^{40}K for all the 15 rock samples are presented in Table 1 and Fig. 2. From Table 1, it is noted that the activity concentration of natural radionuclides varied from one sampling location to another on the same hill which may be due to physical, chemical, and geological variations in the study area (Krmar et al. 2009). The activity concentration ranges for ^{238}U, ^{232}Th, and ^{40}K are between 12.97 and 49.89; 6.4 and 27.05, and 51.85 and 95.84 Bq kg^{-1}, respectively (Table 1). The average concentrations of ^{238}U, ^{232}Th, and ^{40}K were 27.48, 13.90, and 73.82 Bq kg^{-1}, respectively. According to UNSCEAR (2000), the world average values for ^{238}U, ^{232}Th, and ^{40}K are 35, 30, and 400 Bq kg^{-1}, respectively. The obtained values were 1.27 (21.49%), 2.16 (53.67%), and 5.42 (81.55%) times lower than the world mean activity concentrations of ^{238}U, ^{232}Th, and ^{40}K for rock samples (N = 15), respectively. It is to be noted that, apart from the rock samples collected from locations 2, 6, and 9, all the other samples have lower values of ^{238}U than the world average value. Moreover, for ^{232}Th and ^{40}K, the values of all samples were below the world average values. This shows that the radioactive materials are randomly distributed from one location to the other (Harb et al. 2012).

Environmental Impact Assessment of the Radionuclides

To determine the factors relating to health and safety of a person exposed to the environment, there are several methods which are used to calculate the environmental impacts of natural radionuclides. In the present study, the impacts are evaluated in terms of air-absorbed dose rate (D_{AA}), indoor gamma dose rate (D_{IN}), radium equivalent activity index (Ra_{eq}), gamma-ray representative index (Iγ), and excess lifetime cancer risk (ELCR).

Air-Absorbed Dose Rate (D_{AA})

The measured activity concentrations of ^{238}U, ^{232}Th and ^{40}K are converted into doses to calculate the total air-

Table 1 Activity concentration of natural radionuclides (^{238}U, ^{232}Th, and ^{40}K) in rock samples of Kolli hills

S. no.	Activity concentration of radionuclides (Bq kg^{-1})		
	^{238}U	^{232}Th	^{40}K
1	33.47	16.6	72.36
2	42.22	20.94	81.63
3	20.7	9.39	58.87
4	31.84	15.49	69.13
5	12.97	6.4	51.85
6	49.89	27.05	95.84
7	24.28	11.51	67.66
8	30.19	15.63	84.62
9	44.81	21.82	76.86
10	19.91	10.93	77.62
11	16.34	8.69	66.01
12	21	11.97	81.54
13	27.57	15.37	89.39
14	15.24	7.38	69.4
15	21.7	9.4	64.5
Mean	27.48	13.90	73.82
World mean	35	30	400
Variation of calculated mean values with world mean values in %	(−) 21.49	(−) 53.67	(−) 81.55

(−) indicates lower value

absorbed dose rate (D_{AA}) using the conversion factor of 0.462 nGy h^{-1}/Bq kg^{-1} for ^{238}U, 0.604 nGy h^{-1}/Bq kg^{-1} for ^{232}Th, and 0.0417 nGy h^{-1}/Bq kg^{-1} for ^{40}K (UNSCEAR 2000). The external air-absorbed gamma dose rate in air at a height of about 1 m above the ground was calculated by using the given formula:

$$D_{AA}\left(\text{nGy h}^{-1}\right) = 0.462C_U + 0.604C_{Th} + 0.0417C_K. \quad (3)$$

The calculated D values for the 15 rock samples ($N = 15$) of Kolli hills are presented in Table 2. The air-absorbed dose rate of the samples from the study area varied from 12.02 nGy h^{-1} (s. no. 5) to 43.38 nGy h^{-1} (s. no. 6), with a mean value of 24.17 nGy h^{-1}. The D_{AA} values for all the collected samples are below the global mean value of gamma radiation dose level from terrestrial sources, which according to UNSCEAR (2000) is 57 nGy h^{-1}. This mean value is about 2.4 times (57.6%) less than the world mean value. This may be due to the low concentrations of ^{238}U and ^{232}Th in sampling locations.

Indoor Gamma Dose Rate (D_{IN})

When sediments are used as building materials, the indoor gamma dose rate (D_{IN}) due to the emissions of gamma rays from natural radionuclides ^{238}U, ^{232}Th, and ^{40}K was calculated based on the assumption that: (1) the dimension of the room is 4 m × 5 m × 2.8 m; (2) wall thickness is 20 cm; and (3) the density of the aggregates is 2.35 × 10^3 kg m^{-3}. D_{IN} is calculated using the following equation (Turhan and Gündüz 2008; European Commission 1999):

$$D_{IN}\left(\text{nGy h}^{-1}\right) = 0.92C_U + 1.1C_{Th} + 0.080C_k, \quad (4)$$

where C_U, C_{Th}, and C_K are the activity concentrations of radium, thorium, and potassium in Bq kg^{-1}, respectively. The indoor gamma dose rate for the 15 rock samples is shown in Table 2. The calculated minimum and maximum values are 23.12 and 83.32 nGy h^{-1}, respectively, with a mean value of 46.48 nGy h^{-1}. This mean value is 1.8 times lower than the worldwide mean value (84 nGy h^{-1}) (UNSCEAR 2000).

Radium Equivalent Activity Index (Ra_{eq})

The natural radioactivity rocks, sediments, and soil are not uniform throughout the world. The uniformity with respect to exposure to radiation has been defined in terms of radium equivalent activity (Ra_{eq}) in Bq kg^{-1} to compare the specific activity of materials containing different amounts of ^{238}U, ^{232}Th, and ^{40}K using a single quantity and is given by the following relation (Beretka and Mathew 1985):

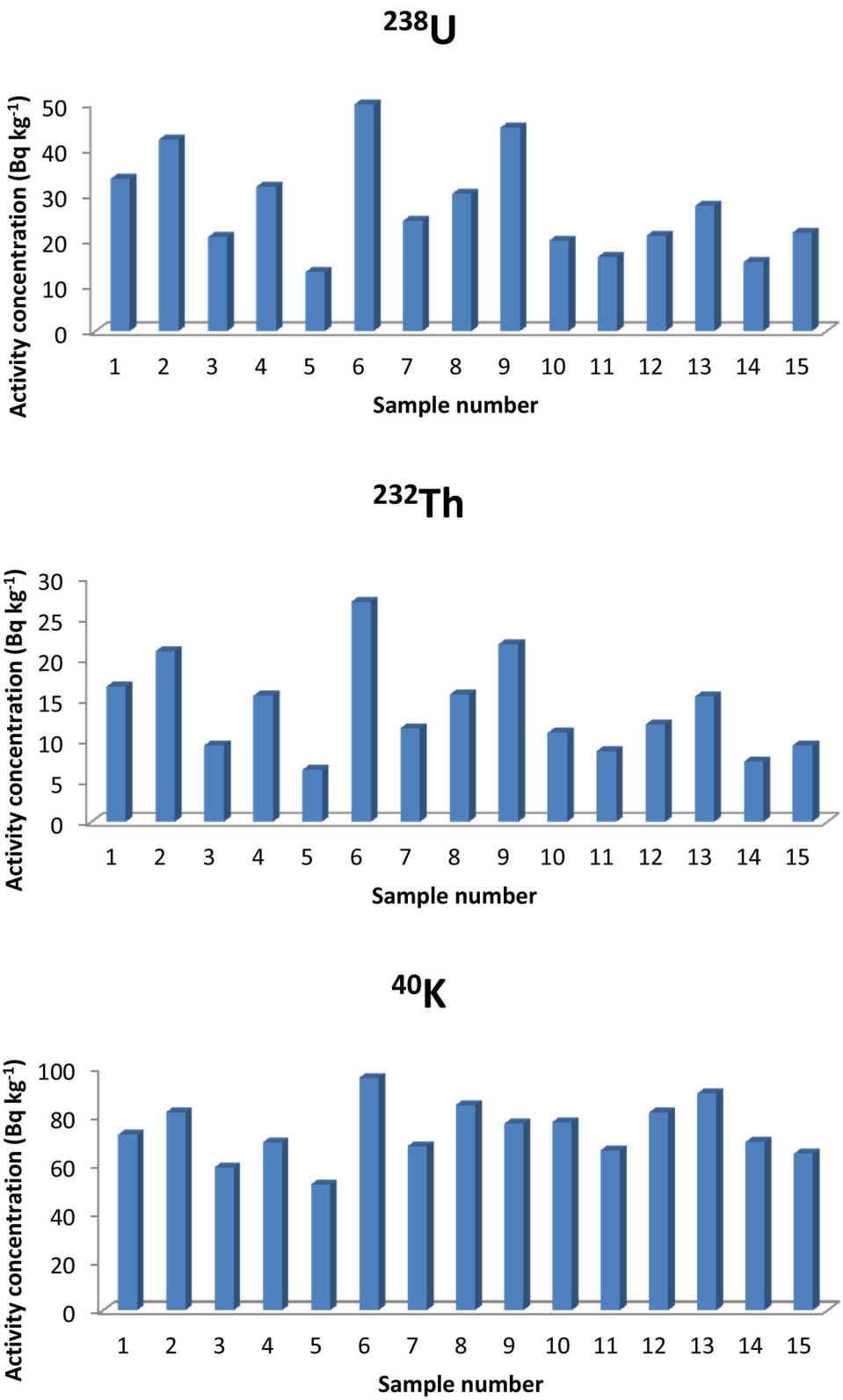

Fig. 2 Distribution of activity concentration of natural radionuclides (^{238}U, ^{232}Th, and ^{40}K) in rock samples of Kolli hills

$$Ra_{\mathrm{eq}}\left(\mathrm{Bq\ kg^{-1}}\right) = C_{\mathrm{U}} + 1.43C_{\mathrm{Th}} + 0.077C_{\mathrm{K}}, \quad (5)$$

where C_{U}, C_{Th}, and C_{K} are the activity concentrations of ^{238}U, ^{232}Th, and ^{40}K in Bq kg^{-1}, respectively. It has been assumed that 370 Bq kg^{-1} ^{238}U, 259 Bq kg^{-1} ^{232}Th, or 4810 Bq kg^{-1} ^{40}K produces the same gamma dose rate (Krisiuk et al. 1971), when Ra_{eq} is defined for the collected samples. The calculated Ra_{eq} values for all the collected

Table 2 Radiation hazard parameters (D_{AA}, D_{IN}, Ra_{eq}, I_γ, and ELCR) in rock samples of Kolli hills

S. no.	Air-absorbed dose rate (D_{AA}) nGy h^{-1}	Indoor gamma dose rate (D_{IN}) nGy h^{-1}	Radium equivalent activity (Ra_{eq}) (Bq kg^{-1})	Gamma-ray index (I_γ)	Excess life time cancer risk ELCR ($\times 10^{-3}$)
1	28.51	54.84	62.78	0.44	0.12
2	35.56	68.41	78.45	0.55	0.15
3	17.69	34.08	38.66	0.27	0.08
4	26.95	51.86	59.31	0.41	0.12
5	12.02	23.12	26.11	0.19	0.05
6	43.38	83.32	95.95	0.67	0.19
7	20.99	40.41	45.95	0.32	0.09
8	26.92	51.74	59.06	0.41	0.12
9	37.09	71.38	81.93	0.57	0.16
10	19.04	36.55	41.52	0.29	0.08
11	15.55	29.87	33.85	0.24	0.07
12	20.33	39.01	44.4	0.31	0.09
13	25.75	49.42	56.43	0.4	0.11
14	14.39	27.69	31.14	0.22	0.06
15	18.39	35.46	40.11	0.28	0.08
Mean	24.17	46.48	53.04	0.37	0.10
Minimum	12.02	23.12	26.11	0.19	0.05
Maximum	43.38	83.32	95.95	0.67	0.19
Median	20.99	40.41	45.95	0.32	0.09
Standard deviation	8.74	16.8	19.51	0.14	0.04
Skewness	0.68	0.68	0.68	0.71	0.67

samples are presented in Table 2. The values of Ra_{eq} varied from 26.11 to 95.95 Bq kg^{-1} with an average value of 53.04 Bq kg^{-1}. According to Krisiuk et al. (1971), if $Ra_{eq} < 370$ Bq kg^{-1}, then the external dose rate will be below 1.5 mSv $year^{-1}$ and this determines the safe utility of materials. The calculated average value of Ra_{eq} in rock samples of the Kolli hills is lower than the maximum permissible value of 370 Bq kg^{-1} suggested for building materials from the point of radiation hazard (OECD 1979; Iqbal et al. 2000).

Gamma-Ray Representative Level Index (I_γ)

The estimation of radiation hazards in building materials, which are associated with natural radionuclides, is done by means of gamma-ray representative index. It is defined by the following equation (Mantazul et al. 1999):

$$I_\gamma = \frac{C_U}{150} + \frac{C_{Th}}{100} + \frac{C_K}{1500}. \quad (6)$$

where C_U, C_{Th}, and C_K are the activity concentrations of ^{238}U, ^{232}Th, and ^{40}K in Bq kg^{-1}, respectively. European Commission (1999) has introduced two criteria for materials which are used as building materials, i.e., an exemption criterion of 0.3 mSv y^{-1} and an upper limit of 1 mSv y^{-1} for building materials such as rocks when they are used in large quantities; an exemption dose criterion of 0.3 mSv y^{-1} corresponds to $I_\gamma \leq 0.5$, whereas the dose criterion of 1 mSv y^{-1} corresponds to $I_\gamma \leq 1$. For materials such as tiles, the corresponding I_γ value must be between 2 and 6. Building material with I_γ exceeding 6 corresponds to a dose rate of > 1 mSv y^{-1} (European Commission 1999) and should be totally avoided for the purpose of construction. According to UNSCEAR (1993) report, this is the maximum value of dose rate in air recommended for humans living in a particular region.

The calculated values of I_γ for all the 15 rock samples are listed in Table 2. It is noted from Table 2 that the I_γ values are between 0.19 and 0.67 with an average value of 0.37. It must be taken into account that samples collected from locations 2, 6, and 9 have $I_\gamma > 0.5$, whereas all the other samples have $I_\gamma < 0.5$. This indicates that rock samples of Kolli hills that do not expose any risk can be widely used for the construction of buildings.

Excess Lifetime Cancer Risk (ELCR)

The excess lifetime cancer risk (ELCR) for the rock samples of Kolli hills was calculated using the following equation:

$$\text{ELCR}\left(\times 10^{-3}\right) = \text{AEDE} \times \text{DL} \times \text{RF}, \quad (7)$$

where AEDE is the annual effective dose equivalent (in mSv y^{-1}), DL is the duration of life (on an average of 70 years), and RF is the risk factor, i.e., fatal cancer risk per Sievert (in Sv^{-1}), respectively. For the public, ICRP 60 uses values of 0.05 for the purpose of stochastic effects (Taskin et al. 2009). The calculated values of ELCR for all the sediment samples are clearly presented in Table 2. As seen from Table 2, the calculated minimum and maximum ELCR values are 0.05 and 0.19, respectively. Moreover, it is noted that the average of the 15 rock samples is 0.10×10^{-3}, and this value is 2.9 times lower than that of the recommended worldwide average value of 0.29×10^{-3} (UNSCEAR 2000).

Magnetic Properties

Values of χ ranged from 33.1 to 510.7 $\times$ 10^{-8} m^3 kg^{-1}. Specific susceptibility is a magnetic concentration-dependent parameter, and its values vary according to the kind of

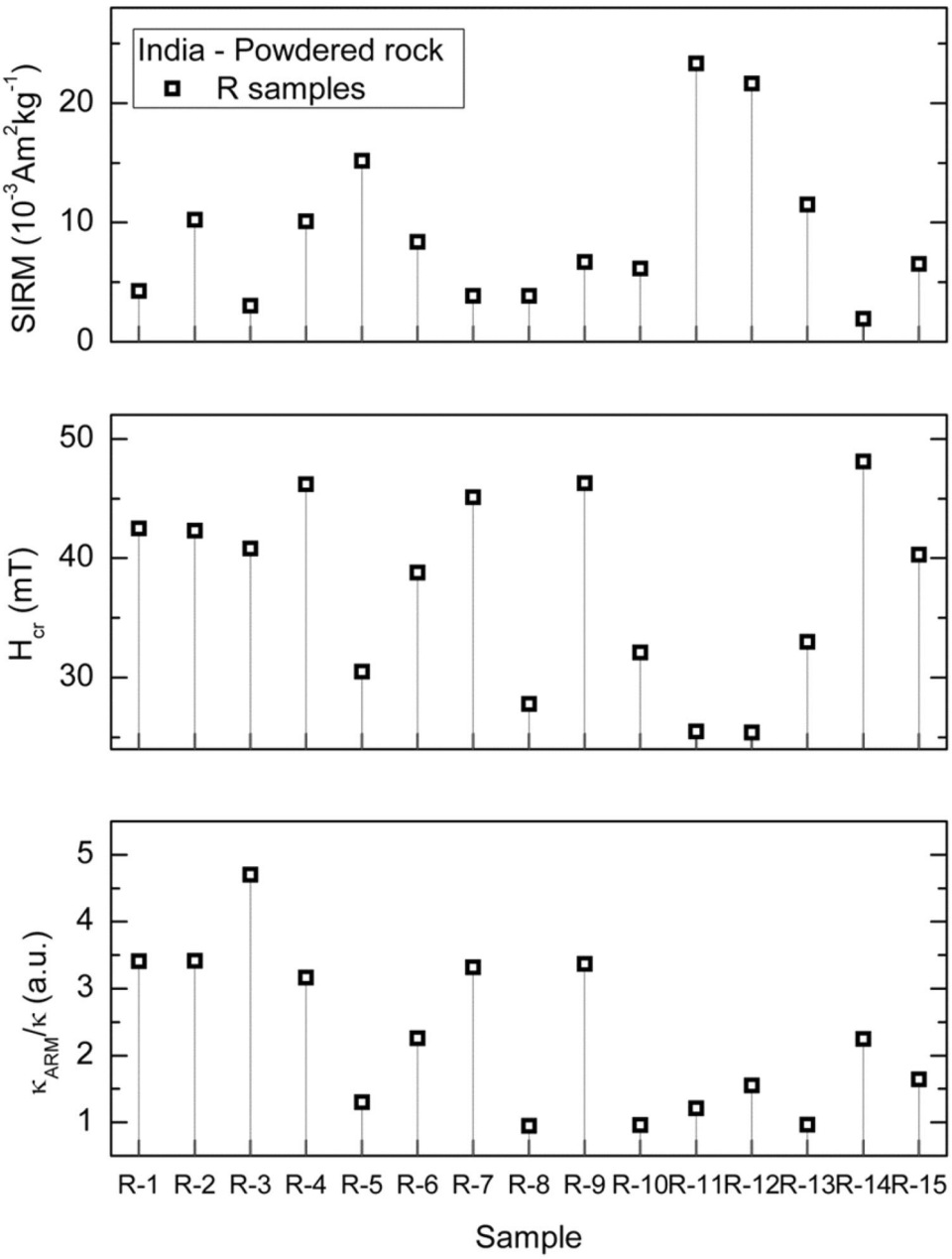

Fig. 3 Spatial distribution of magnetic concentration-dependent parameter χ, mineral-dependent parameter H_{cr}, and magnetic grain size-dependent parameter κ_{ARM}/κ for Kolli hills (India)

materials, i.e., diamagnetic ($\sim -6 \times 10^{-9}$ m^3 kg^{-1}), paramagnetic ($\sim 10^{-6}$ m^3 kg^{-1}), and ferrimagnetic materials ($\sim$ 0.5–5.6 $\times 10^{-3}$ m^3 kg^{-1}, in detail in Maher et al. (1999). The other concentration-related remanent parameters varied between 40.5 and 436.2 $\times 10^{-6}$ Am^2 kg^{-1} for ARM, and between 2.0 and 23.3 $\times 10^{-3}$ Am^2 kg^{-1} for SIRM (Fig. 3, Table 3).

Measurements of isothermal remanent magnetization acquisition (and backfield) revealed the dominance of ferrimagnetic carriers for most of the samples (Table 3). This fact is especially concluded from *S*-ratio results, which varied between 0.827 and 1. *S*-ratio values clearly show the predominance of ferrimagnetic minerals over antiferromagnetic minerals.

Parameter χ correlates significantly with SIRM ($R = 0.95$, $p < 0.01$) indicating that ferrimagnetic minerals dominate the magnetic signal as well. Both parameters are represented in Fig. 4, which show a linear trend and allow to identify rock samples with a higher magnetic concentration (SIRM $> 11.5 \times 10^{-3}$ Am^2 kg^{-1}), that is, sample nos. 5, 11, 12, and 13.

Remanent coercivity values varied widely between 25.4 and 48.1 mT (Fig. 3), and most of samples belong to two characteristic intervals: 25.4–33.0 mT (sample nos. 5, 8, 10, 11, 12, and 13) and 40.3–48.1 mT (sample nos. 1, 2, 3, 4, 7, 9, 14, and 15). This H_{cr} range corresponds to values of magnetite-like mineral with different characteristics. An extra contribution of antiferromagnetic materials could be expected in samples with higher H_{cr}. In addition, this variation can be interpreted as the contribution of different magnetite particles with a wider grain size distribution range, which is supported by significant correlations between this parameter and grain size-dependent ARM/SIRM ($R = 0.65$, $p < 0.01$), κ_{ARM}/κ ($R = 0.73$, $p < 0.01$). Values of SIRM/χ, from 4.6 to 10.1 kA/m, belong to the range of (titano) magnetite (Peters and Dekkers 2003), and higher values can be interpreted as finer magnetic grain size abundance (correlation with κ_{ARM}/κ is $R = 0.69$, $p < 0.01$). Both magnetic parameters are displayed in a biplot (Fig. 5). Two groupings are identified as mentioned for parameter H_{cr} above.

The κ_{FD}% parameter is sensible to the presence of superparamagnetic (SP) material (Dearing et al. 1996). Values of $\kappa_{FD}\% > 2.0\%$ indicate virtually no SP grains, between 2.0 and 10.0% indicate admixture of SP and coarser non-SP grains, between 10.0 and 14.0% indicate virtually all SP grains. In these powdered rock samples, the κ_{FD}% mean value is 0.2% and the standard deviation (SD) is 0.6%. The presence of SP grains can be discarded.

Magnetic grain size-dependent parameters, i.e., ARM/SIRM, κ_{ARM}/κ (Fig. 3), and the King's plot show the presence of coarser magnetic grain size for most of samples with higher concentration (sample nos. 5, 11, 12, and 13). This trend can be appreciated in Fig. 6; higher values of χ correspond to coarser magnetic grain sizes (at about 5 and 20 μm). Values of magnetic parameter κ_{ARM}/κ are displayed in Fig. 3. It can be appreciated that higher values are indicative of finer magnetic grains. In particular, κ_{ARM}/κ values above 3.0 correspond to magnetic grain sizes between 0.2 and 1 μm, and group samples with low magnetic concentration-dependent values such as nos. 1, 2, 3, 4, 7, 9, and 14 (Fig. 3). On the other hand, sample nos. 5, 8, 10,

Table 3 Magnetic parameters of rock samples from Kolli hills, India

Sample no.	χ, 10^{-8} m^3 kg^{-1}	χ_{ARM}, 10^{-8} m^3 kg^{-1}	ARM, 10^{-6} A m^2 kg^{-1}	SIRM, 10^{-3} A m^2 kg^{-1}	κ_{FD}, %	κ_{ARM}/κ, a.u.	ARM/SIRM, a.u.	SIRM/χ, kA/m	H_{cr}, mT	*S* ratio, a.u.
1	60.4	206	150.3	4.3	− 0.2	3.4	0.035	7.1	42.5	0.903
2	111.3	379.8	267.7	10.2	1.4	3.4	0.026	9.2	42.3	0.939
3	34.5	162.2	105.7	3	0	4.7	0.035	8.8	40.8	0.958
4	99.8	315.5	225.2	10.1	0.8	3.2	0.022	10.1	46.2	0.862
5	292.9	381.6	264.7	15.2	0	1.3	0.017	5.2	30.5	1
6	87.7	198.1	141.2	8.4	0.3	2.3	0.017	9.5	38.8	0.968
7	44.8	148.7	109.1	3.9	− 0.7	3.3	0.028	8.6	45.1	0.913
8	79.9	75.8	51	3.9	− 0.5	0.9	0.013	4.8	27.8	0.919
9	75.5	254.7	185.1	6.7	0.8	3.4	0.028	8.9	46.3	0.87
10	78.7	75.7	40.5	6.2	− 0.2	1	0.007	7.8	32.1	0.929
11	510.7	618.9	436.2	23.3	0.6	1.2	0.019	4.6	25.5	0.982
12	330.3	513.7	357.4	21.6	0.2	1.6	0.017	6.6	25.4	0.996
13	224.7	217.7	149.2	11.5	0.4	1	0.013	5.1	33	0.973
14	33.1	74.5	51.6	2	− 0.3	2.2	0.026	5.9	48.1	0.863
15	81.5	134.3	96.4	6.5	− 0.1	1.6	0.015	8	40.3	0.827

11, 12, 13, and 15 show κ_{ARM}/κ values below 1.6 corresponding to the coarsest magnetic grains of 5–20 μm (Figs. 3, 6).

Multivariate Statistical Analysis

Pearson's correlation analysis was carried to understand the relation between the activity concentration of natural radionuclides (^{238}U, ^{232}Th, and ^{40}K), radioactive hazard parameters (D_{AA}, D_{IN}, Ra_{eq}, I_γ, and ELCR), and the various magnetic variables (Table 4). From Table 4, statistically significant positive correlation among the activity concentration of U and Th (0.986); U and K (0.663); Th and K (0.757) is observed. This indicates that all the three radionuclides contribute to the activity concentration in Kolli hill's rock samples. Also, it is noted that U and Th correlate higher than U and K and also between Th and K. This indicates that the activity concentration of any one of the radionuclide among the two can be used to predict the activity concentration of the other radionuclide. This is in good agreement with the findings of Okedeyi et al. (2014). As observed from Table 4, the strong positive correlation coefficient between ^{238}U and ^{232}Th may be due to the fact that uranium and thorium decay series occur together in nature (Tanaskovic et al. 2012). Moreover, the derived radioactive hazard parameters (D_{AA}, D_{IN}, Ra_{eq}, I_γ, and ELCR) are also showing strong correlation with ^{232}Th and ^{238}U. This indicates that ^{238}U and ^{232}Th contribute greatly for the hazard parameters in Kolli hill's rock samples. Medium correlation is observed between ^{40}K with ^{232}Th and ^{238}U, while ^{232}Th shows slightly higher correlation. But magnetic susceptibility (χ) and its other related parameters (χ_{ARM}, ARM, SIRM, κ_{FD}%, κ_{ARM}/κ, ARM/SIRM, SIRM/χ, H_{cr}, S-ratio) show poor correlation with all the radioactive observations. In the present study, the strong correlations of ^{238}U and ^{232}Th among themselves and with other radiological parameters indicate that they greatly contribute to the emission of gamma radiation in all the locations, whereas the poor correlation with magnetic susceptibility indicates that no such correlation to natural radioactivity exists in the rock samples of Kolli hills (Nagamalleswara Rao 1995). But, it is to be considered that, a near-positive correlation that was also observed between κ_{FD}% and U (0.481), κ_{FD}% and Th (0.471), and also between κ_{FD}% and dose rate D (0.472), SIRM/χ correlates significantly (p value < 0.05) with U, Th, and to the derived radioactive parameters D_{AA}, D_{IN}, Ra_{eq}, I_γ, and ELCR (R = 0.501–0.578). This shows that the grain size dependence parameter also plays a significant role in increasing the activity concentration of U, Th, and various calculated hazard parameters.

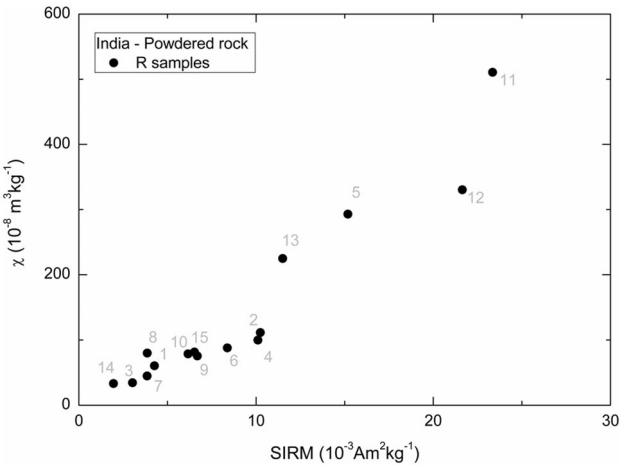

Fig. 4 Biplot of magnetic concentration-dependent parameters, magnetic susceptibility (χ), and remananent magnetization (SIRM)

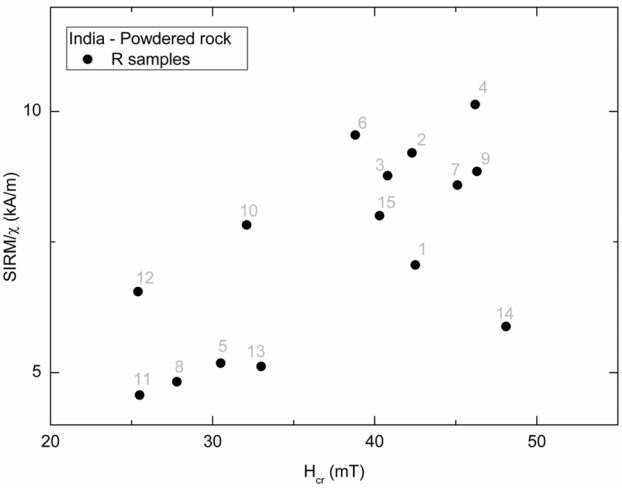

Fig. 5 Biplot of magnetic mineral-dependent parameters SIRM/χ and H_{cr}

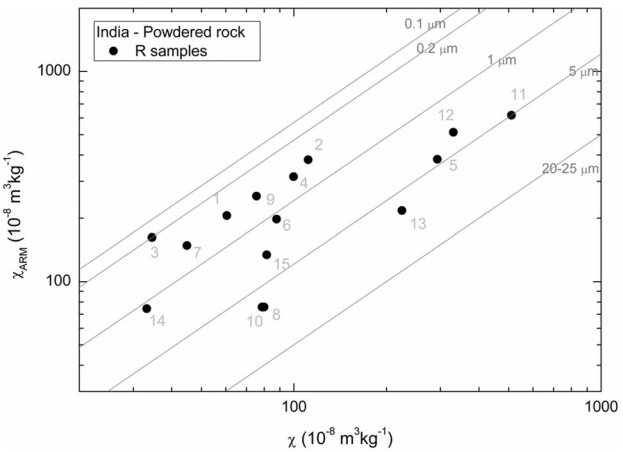

Fig. 6 The King's plot (χ_{ARM} versus χ) for rock-powered samples from Kolli hills

Table 4 Pearson's coefficient among the activity concentration of natural radionuclides (^{238}U, ^{232}Th, and ^{40}K), radiological hazard parameters, and magnetic parameters

	^{238}U	^{232}Th	^{40}K	D_{AA}	D_{IN}	Ra_{eq}	I_γ	ELCR	χ	χ_{ARM}	ARM	SIRM	κ_{FD} %	κ_{ARM}/κ	ARM/SIRM	SIRM/χ	H_{cr}	S ratio
^{238}U	1.000																	
^{232}Th	**0.986**	1.000																
^{40}K	**0.663**	**0.757**	1.000															
D_{AA}	**0.995**	**0.997**	**0.730**	1.000														
D_{IN}	**0.995**	**0.997**	**0.729**	**1.000**	1.000													
Ra_{eq}	**0.995**	**0.997**	**0.728**	**1.000**	**1.000**	1.000												
I_γ	**0.994**	**0.998**	**0.729**	**1.000**	**1.000**	**1.000**	1.000											
ELCR	**0.992**	**0.996**	**0.731**	**0.998**	**0.998**	**0.998**	**0.997**	1.000										
χ	− 0.372	− 0.289	− 0.108	− 0.332	− 0.334	− 0.331	− 0.323	− 0.318	1.000									
χ_{ARM}	− 0.090	− 0.052	− 0.125	− 0.078	− 0.079	− 0.077	− 0.071	− 0.067	**0.862**	1.000								
ARM	− 0.067	− 0.032	− 0.122	− 0.058	− 0.058	− 0.056	− 0.050	− 0.047	**0.851**	**0.999**	1.000							
SIRM	− 0.221	− 0.140	− 0.011	− 0.182	− 0.184	− 0.181	− 0.175	− 0.168	0.951	**0.926**	**0.916**	1.000						
κ_{FD} %	***0.481***	***0.471***	0.218	***0.472***	***0.472***	***0.473***	***0.477***	***0.469***	0.289	**0.585**	**0.589**	0.438	1.000					
κ_{ARM}/κ	0.370	0.261	− 0.226	0.302	0.304	0.304	0.298	0.300	− 0.511	− 0.098	− 0.081	− 0.423	0.210	1.000				
ARM/SIRM	0.185	0.083	− 0.342	0.120	0.122	0.122	0.120	0.112	− 0.337	− 0.001	0.020	− 0.342	0.073	**0.894**	1.000			
SIRM/χ	**0.578**	**0.501**	0.088	**0.532**	**0.534**	**0.533**	**0.524**	**0.534**	− 0.578	− 0.189	− 0.176	− 0.360	0.322	**0.708**	0.361	1.000		
H_{cr}	0.368	0.252	− 0.128	0.302	0.305	0.303	0.298	0.282	− 0.739	− 0.447	− 0.421	− 0.673	0.088	**0.730**	**0.640**	**0.670**	1.000	
S ratio	− 0.151	− 0.035	0.129	− 0.093	− 0.096	− 0.093	− 0.081	− 0.086	**0.635**	**0.530**	**0.506**	**0.616**	0.106	− 0.258	− 0.209	− 0.383	− 0.704	1.000

Bold values indicate positive correlation among the variables (> 0.5). Bold italic values indicate near positive correlation among the variables (∼ 0.5)

Table 5 Clusters of rock samples with similar activity features obtained from a nonhierarchical *k*-means clustering analysis

Variable (Bq kg^{-1})	Mean overall	Cluster A1 ($n = 6$)		Cluster A2 ($n = 6$)		Cluster A3 ($n = 3$)	
		Samples 3, 5, 7, 11, 14, 15		Samples 1, 4, 8, 10, 12, 13		Samples 2, 6, 9	
		Mean group	*p* value	Mean group	*p* value	Mean group	*p* value
^{238}U	27.48	18.53	1.1E−02	–	–	45.64	1.7E−03
^{232}Th	13.90	8.80	6.0E−03	–	–	23.27	2.1E−03
^{40}K	73.87	63.04	3.0E−03	–	–	–	–

Table 6 Clusters of rock samples with similar magnetic features obtained from a nonhierarchical *k*-means clustering analysis

Variable	Mean overall	Cluster M1 ($n = 5$)		Cluster M2 ($n = 7$)		Cluster M3 ($n = 3$)	
		Samples 8, 10, 13, 14, 15		Samples 1, 2, 3, 4, 6, 7, 9		Samples 5, 11, 12	
		Mean group	*p* value	Mean group	*p* value	Mean group	*p* value
χ (10^{-8} m^3 kg^{-1})	143.1	–	–	–	–	378.0	8.9E−04
SIRM (10^{-3} Am^2 kg^{-1})	9.1	–	–	–	–	20.0	1.1E−03
ARM (10^{-6} Am^2 kg^{-1})	175.4	77.7	2.0E−02	–	–	352.8	3.0E−03
κ_{ARM}/κ (a.u)	2.3	1.3	2.7E−02	3.4	9.2E−04	–	–
ARM/SIRM (a.u.)	0.02	0.01	3.0E−02	0.03	7.5E−03	–	–
H_{cr} (mT)	37.7	–	–	43.1	1.2E−02	27.1	1.0E−02
SIRM/χ (kA/m)	7.4	–	–	8.9	2.8E−03	–	–

From the cluster analysis (CA), two independent CAs were obtained for magnetic parameters on one hand, and on the other hand, for activity concentration of radionuclides. Both magnetic- and radionuclide-related variables are not statistically correlated for this study case. Three clusters for each kind of variables are detailed in Tables 5 and 6.

Sample nos. 3, 5, 7, 11, 14, and 15 belong to the Cluster A1 with the lowest activity concentration of radionuclides (Table 5). On the contrary, sample nos. 2, 6, and 9 are grouped in Cluster A3 that has mean group values (45.64 and 23.27 Bq kg^{-1} for ^{238}U and ^{232}Th, respectively) higher than the mean overall variable values (27.48 and 13.90 Bq kg^{-1} for ^{238}U and ^{232}Th, respectively). Thus, only sample nos. 2, 6, and 9 have values of ^{238}U higher than the world average value (UNSCEAR 2000) and may be discarded for construction purposes.

The multivariate analysis for magnetic variables involved concentration, grain size, and mineralogy-dependent parameters, which is observed in Table 6. The first group (Cluster M1, sample nos. 8, 10, 13, 14, and 15) is characterized by low magnetic concentration (ARM = 77.7 × 10^{-6} Am^2 kg^{-1}) and coarser magnetic grains (i.e., lower values of ratios κ_{ARM}/κ and ARM/SIRM). The second group (Cluster M2, sample nos. 1, 2, 3, 4, 6, 7, and 9) shows concentration values statistically similar to the mean overall, but it is characterized by finer magnetic grains (i.e., higher values of ratios κ_{ARM}/κ and ARM/SIRM) and higher coercivity values than the mean overall. On the other hand, Cluster M3 (sample nos. 5, 11, and 12) is statistically different from the mean overall by their high magnetic concentration (χ = 378.0 × 10^{-8} m^3 kg^{-1}, SIRM = 20.0 × 10^{-6} Am^2 kg^{-1}, and ARM = 77.7 × 10^{-6} Am^2 kg^{-1}) and magnetic mineralogy evidencing low-coercivity minerals (H_{cr} = 27.1 mT, Table 6).

From the magnetic point of view, samples from Cluster M3 and Cluster M2 may be more appropriated for construction purposes. These samples (nos. 5, 11, and 12; and nos. 1, 2, 3, 4, 6, 7, and 9) have higher magnetic concentration, and therefore, higher ferromagnetic mineral contents (iron oxides) in these samples improve the properties of concrete for construction purposes.

Conclusion

Using gamma-ray spectroscopy, the natural radioactivity levels of ^{238}U, ^{232}Th, and ^{40}K have been measured for the rock samples collected from various altitudes of Kolli hills in the Eastern Ghats of India. The activity concentrations ranged between 12.97 and 49.89 Bq kg^{-1} for ^{238}U, 6.4 and

27.05 Bq kg^{-1} for ^{232}Th, and 51.85 and 95.84 Bq kg^{-1} for ^{40}K. The mean concentrations of ^{232}U (27.48 Bq kg^{-1}), ^{232}Th (13.90 Bq kg^{-1}), and ^{40}K (73.82 Bq kg^{-1}) are 21.49, 53.67, and 81.55% lower than the worldwide average values of 35, 30, and 400 Bq kg^{-1}, respectively. The calculated mean air-absorbed dose rate is 24.17 nGy h^{-1}, which is 57.59% lower than the world recommended mean value of 57 nGy h^{-1}. All the derived radiological parameters (D_{AA}, D_{IN}, Ra_{eq}, I_{γ}, and ELCR) have mean values lower than that of the permissible global values. This confirms that the rock samples of Kolli hills emit low level of natural radionuclides and can be extensively used for building construction purposes. Magnetic properties of the samples indicate that ferrimagnetic minerals are the main magnetic carriers of Kolli hill's rocks. Among the magnetic minerals, magnetite with grain sizes between 0.2 and 20 μm are identified from parameters H_{cr} (25.4–48.1 mT), κ_{ARM}/κ (0.9–4.7), as well as plots SIRM/χ versus H_{cr} and χ_{ARM} versus χ. From Pearson's correlation analysis, the present study confirms that U, Th, K, and SIRM/χ contribute greatly, whereas, grain size dependence parameter κ_{FD}% plays a significant role in the various radiological hazard parameters of Kolli hill's rock samples. The multivariate analysis of activity concentration of radionuclides indicates that most of the samples (Clusters A1 and A2) have lower activity than the world average value, except sample nos. 2, 6, and 9 for ^{238}U (Cluster A3). The cluster analysis using magnetic properties, such as concentration, mineralogy, and grain sizes, outcomes three clusters of samples where Clusters M3 and M2 have higher magnetic concentration (e.g., SIRM = 20.0×10^{-3} Am^2 kg^{-1}) and low-coercivity minerals (e.g., H_{cr} = 27.1 mT), and therefore, higher ferrimagnetic mineral contents in sample nos. 4, 5, 11, and 12 improve the properties of concrete if used for construction purposes.

Acknowledgements The authors thank the Head and staff of the Physics Department, Gulbarga University, for their help in gamma-ray analysis. The authors also thank the Universidad Nacional del Centro de la Provincia de Buenos Aires (UNCPBA), and the National Council for Scientific and Technological Research (CONICET).

References

Bartington Instruments Ltd. (1994) Operation manual. Environmental magnetic susceptibility—using the Bartington MS2 system. Chi Publishing, Kentworth, p 54

Beretka J, Mathew P (1985) Natural radioactivity of Australian building materials, industrial waste and byproducts. Health Phys 48:87–95

Chaparro MAE, Gargiulo JD, Irurzun MA, Chaparro MAE, Lecomte KL, Böhnel HN, Córdoba FE, Vignoni PA, ManograssoCzalbowski NT, Lirio JM, Nowaczyk NR, Sinito AM (2014) El uso de parámetrosmagnéticos en estudiospaleolimnológicos en Antártida "Magnetic parameters in paleolimnological studies in Antarctica". Latin Am J Sedimentol Basin Anal 21(2):77–96

Dearing J, Dann R, Hay K, Lees J, Loveland P, Maher B, O'Grady K (1996) Frequency-dependent susceptibility measurements of environmental materials. Geophys J Int 124:228–240

Dunlop DJ, Özdemir Ö (1997) Rock magnetism, fundamentals and frontiers. Cambridge University Press, Cambridge, p 573

European Commission (EC) (1999) Radiological protection principles concerning the natural radioactivity of building materials. Radiation protection report no. 112. Directorate-general for environment, nuclear safety and civil protection

Gbadebo AM (2011) Natural radionuclides distribution in the granitic rocks and soils of abandoned quarry sites, Abeokuta, Southwestern Nigeria. Asian J Appl Sci 4:176–185

Gurugnanam B (2015) Analysis of digital elevation model of Kolli hill, south India using shuttle radar topography mission data and GIS techniques. Int J Remote Sens & Geosci 4(6):39–41

Gurugnanam B, Kalaivanan K, Bairavi S (2014) Detailed geomorphic mapping using remote sensing & GIS in Kolli Hill, South India. Int J Sci Res Dev 2(10):803–805

Harb S, El-Kamel AH, Zahran AM, Abbady A, As-Subaihi FAA (2012) Measurement of natural radioactivity in beach sediments from Aden coast on Gulf of Aden, south of Yemen. XI Radiation Physics and Protection Conference, Cairo, Egypt, pp 25–28

Iqbal M, Tufail M, Mirza SM (2000) Measurement of natural radioactivity in marble found in Pakistan using a NaI(Tl) gamma-ray spectrometer. J Environ Radioact 51(2):255–265

King J, Banerjee SK, Marvin J, Özdemir Ö (1982) A comparison of different magnetic methods for determining the relative grain size of magnetite in natural materials: some results from lake sediments. Earth Planet Sci Lett 59:404–419

Krisiuk EM, Tarasov SI, Shamov VP, Shlak NI, Lisachenko EP, Gomelsky LG (1971) A study of radioactivity in building materials. Research Institute for Radiation Hygiene, Leningrad

Krmar M, Slivka J, Varga E, Bikit I, Veskovic M (2009) Correlations of natural radionuclides in sediment from Danube. J Geochem Explor 100(1):20–24

Kumaresan N, Ilango K, Gopinath LR, Bhuvaneswari R, Archaya S (2016) Dynamics of plant hoppers diversity in Kolli Hills, Tamilnadu, India. Int J Fauna Biol Stud 3(1):93–97

Kurnaz A, Kucukomeroglu B, Keser R, Okumusoglu NT, Orkmaz F, Karahan G (2007) Determination of radioactivity levels and hazards of soil and sediment samples in Firtina valley (Rize, Turkey). Appl Radiat Isot 65:1281–1289

Maher BA, Thompson R, Hounslow MW (1999) Introduction. In: Maher BA, Thompson R (eds) Quaternary climate, environments and magnetism. Cambridge University Press, Cambridge, pp 1–48

Mantazul I, Chowdhury M, Alam MN, Hazari SKS (1999) Distribution of radionuclides in the river sediments and coastal soils of Chittagong, Bangladesh and evaluation of the radiation hazard. Appl Radiat Isot 51(6):747–755

Nagamalleswara Rao B (1995) Radiometric, magnetic susceptibility and mineralogical studies in some Beach places of Andhra Pradesh, East coast of India. J Geol Soc India 43:669–675

OECD (Organization of Economic Co-operation and Development) (1979) Exposure to radiation from natural radioactivity in building materials. Report by a Group of Experts of the OECD Nuclear Energy Agency, Paris

Okedeyi AS, Gbadebo AM, Mustapha AO (2014) Effects of physical and chemical properties on natural radionuclides level in soil of quarry sites in Ogun State, Nigeria. J Appl Sci 14(7):691–696

Olarinoye IO, Sharifat Baba-Kutiga AN, Kolo MT, Aladeniyi K (2010) Measurement of background gamma radiation level at two tertiary institutions in Minna, Nigeria. J Appl Sci Environ Manag 14:59–62

Peters C, Dekkers MJ (2003) Selected room temperature magnetic parameters as a function of mineralogy, concentration and grain size. Phys Chem Earth 28:659–667

R Core Team (2017) R: a language and environment for statistical computing. R foundation for statistical computing, Vienna.Version 3.4.3. https://www.R-project.org/. Accessed 25 Jan 2018

Ramasamy V, Suresh G, Venkatachalapathy R, Ponnusamy V, Meenakshisundaram V (2010) Magnetic susceptibility and radiological hazardous nature of the river sediments-spectroscopical approach. Acta Phys Polonica A 118(4):701–711

Tanaskovic I, Golobocanin D, Miljevic N (2012) Multivariate statistical analysis of hydro chemical and radiological data of Serbian spa waters. J Geochem Explor 112:226–234

Taskin H, Karavus M, Ay P, Topuzoglu A, Hindiroglu S, Karahan G (2009) Radionuclide concentrations in soil and lifetime cancer risk due to the gamma radioactivity in Kirklareli, Turkey. J Environ Radioact 100(1):49–53

Thompson R, Oldfield F (1986) Environmental magnetism. Allen & Unwin, London, UK, p 227

Turhan S, Gündüz Lu (2008) Determination of specific activity of 226Ra, 232Th and 40K for assessment of radiation hazards from Turkish pumice samples. J Environ Radioact 99(2):332–342

UNSCEAR (1993) United Nations Scientific Committee on Effects of Atomic Radiation, "Sources and Effects of Ionising Radiation", UNSCEAR Report, New York

UNSCEAR (2000) United Nations Scientific Committee on the Effect of Atomic Radiation. Sources and effects of ionizing radiation. Report to general assembly. United Nations Organization, New York

Verosub KL, Roberts AP (1995) Environmental magnetism: past, present and future. J Geophys Res 100(B2):2175–2192